Human Parvovirus B19 Infection Causes Cell Cycle Arrest of Human Erythroid Progenitors at Late S Phase That Favors Viral DNA Replication

Yong Luo,[a] Steve Kleiboeker,[b] Xuefeng Deng,[a] Jianming Qiu[a]

Department of Microbiology, Molecular Genetics and Immunology, University of Kansas Medical Center, Kansas City, Kansas, USA[a]; Viracor-IBT Laboratories, Lee's Summit, Missouri, USA[b]

Human parvovirus B19 (B19V) infection has a unique tropism to human erythroid progenitor cells (EPCs) in human bone marrow and the fetal liver. It has been reported that both B19V infection and expression of the large nonstructural protein NS1 arrested EPCs at a cell cycle status with a 4 N DNA content, which was previously claimed to be "G_2/M arrest." However, a B19V mutant infectious DNA (M20^{mTAD2}) replicated well in B19V-semipermissive UT7/Epo-S1 cells but did not induce G_2/M arrest (S. Lou, Y. Luo, F. Cheng, Q. Huang, W. Shen, S. Kleiboeker, J. F. Tisdale, Z. Liu, and J. Qiu, J. Virol. 86:10748–10758, 2012). To further characterize cell cycle arrest during B19V infection of EPCs, we analyzed the cell cycle change using 5-bromo-2'-deoxyuridine (BrdU) pulse-labeling and DAPI (4',6-diamidino-2-phenylindole) staining, which precisely establishes the cell cycle pattern based on both cellular DNA replication and nuclear DNA content. We found that although both B19V NS1 transduction and infection immediately arrested cells at a status of 4 N DNA content, B19V-infected 4 N cells still incorporated BrdU, indicating active DNA synthesis. Notably, the BrdU incorporation was caused neither by viral DNA replication nor by cellular DNA repair that could be initiated by B19V infection-induced cellular DNA damage. Moreover, several S phase regulators were abundantly expressed and colocalized within the B19V replication centers. More importantly, replication of the B19V wild-type infectious DNA, as well as the M20^{mTAD2} mutant, arrested cells at S phase. Taken together, our results confirmed that B19V infection triggers late S phase arrest, which presumably provides cellular S phase factors for viral DNA replication.

Human parvovirus B19 (B19V) is a member of the genus *Erythrovirus* within the family *Parvoviridae*. Most commonly, it causes a mild disease called "fifth disease" (1); however, under some conditions, B19V infection can be life threatening (2), e.g., hydrops fetalis in pregnant women (3–5), chronic pure red cell aplasia in immunocompromised patients (6, 7), and transient aplastic crisis in sickle cell disease patients (8–10).

B19V has a single-stranded DNA genome that is flanked by two identical terminal repeats (11). Under a single p6 promoter, the B19V genome expresses one large nonstructural protein (NS1), two small (11-kDa and 7.5-kDa) nonstructural proteins, and two capsid proteins (VP1 and VP2) (12). B19V infection is restricted to human erythroid progenitor cells (EPCs) of human bone marrow and the fetal liver (5, 13–15). Previously, only a few semipermissive cell lines, such as the human megakaryoblastoid cell line UT7/Epo-S1 (16, 17), were found to support B19V replication. Recently, *ex vivo*-expanded human primary CD36$^+$ EPCs, which are differentiated from CD34$^+$ hematopoietic stem cells, have been shown to be highly permissive to B19V infection (18–20). Although B19V replication in UT7/Epo-S1 cells is less efficient (21, 22), the cells can be transfected with a B19V infectious DNA (M20) (23) and produce infectious virions under hypoxic conditions (22).

B19V infection of both UT7/Epo-S1 cells and CD36$^+$ EPCs quickly arrests host cells in a tetraploid state (4 N DNA content) (17, 24, 25), which was previously thought to be "G_2/M arrest." Expression of B19V NS1 *per se* in CD36$^+$ EPCs was identified as capable of inducing EPCs arrested at a 4 N DNA content through deregulation of the E2F family transcription factors (24). However, it is generally accepted that autonomous parvoviruses rely on host cells at S phase for viral DNA amplification (26–32), because of the simplicity of parvovirus genome structures. In addition,

we recently identified a mutant B19V infectious clone DNA (M20^{mTAD2}) that bears mutations in a putative transactivation domain (TAD) of NS1 and replicates efficiently in UT7/Epo-S1 cells but without inducing G_2/M arrest, indicating that G_2/M arrest is dispensable for B19V DNA replication (25). Therefore, we wondered whether B19V infection creates a "pseudo-G_2 phase" environment, as some other DNA viruses do (33).

In this study, we examined the cell cycle change during B19V infection precisely by simultaneously measuring 5-bromo-2'-deoxyuridine (BrdU) incorporation and DNA content. We found that although both B19V infection and NS1 transduction quickly pushed cells into a status with a 4 N DNA content, a large portion of the 4 N cells among the B19V-infected cells, but not among the NS1-transduced cells, still incorporated BrdU. The BrdU incorporation is mainly contributed by cellular DNA synthesis, but not viral DNA replication or cellular DNA repair that is due to DNA damage. More importantly, we observed that several cellular DNA replication regulators were abundant and colocalized with B19V NS1 in the nuclei and that individual knockdown of minichromosome maintenance complex protein 2 (MCM2) and MCM5 significantly impaired B19V DNA replication. Additionally, the B19V-induced S phase arrest was confirmed in transfection of
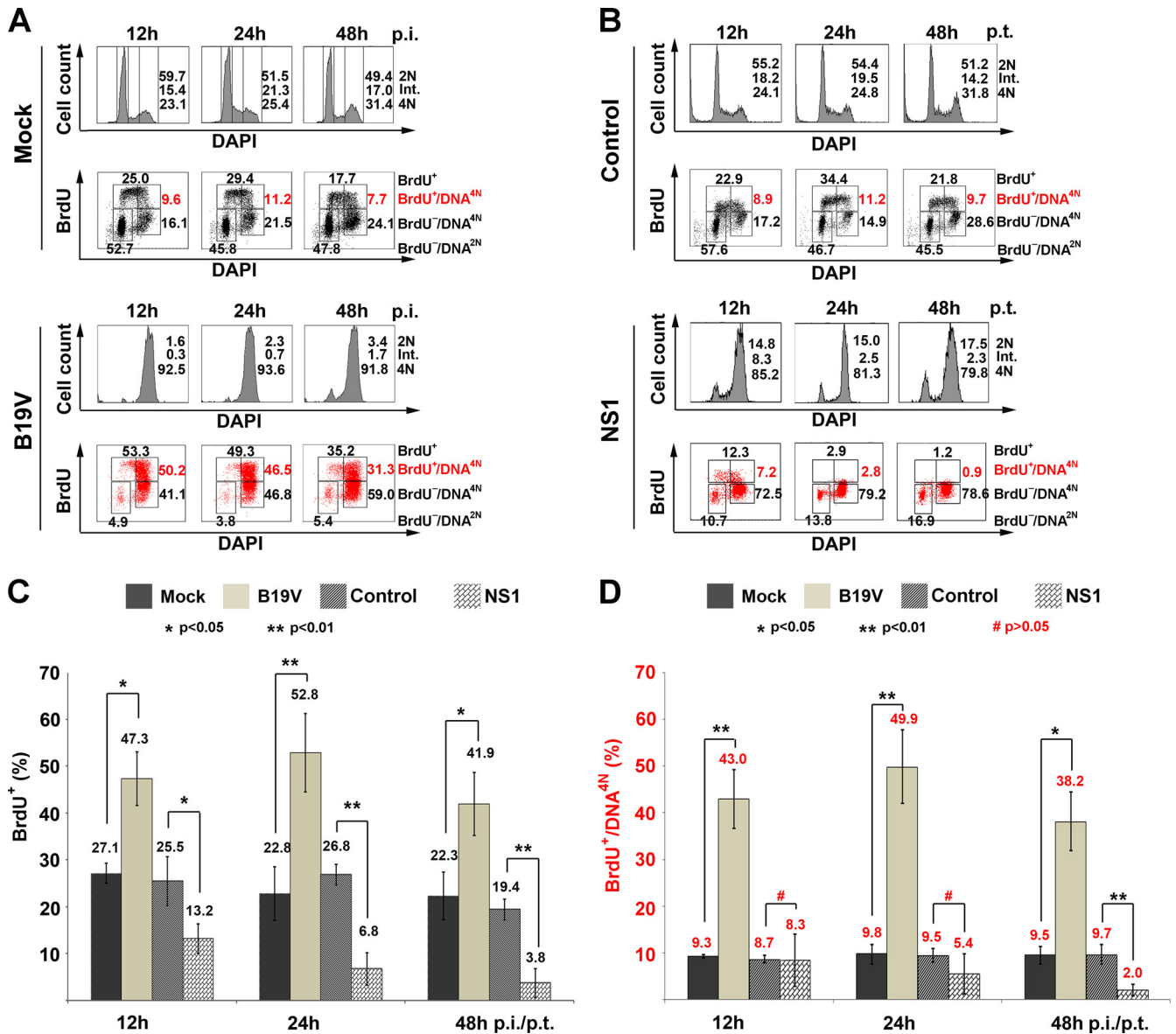
FIG 1 B19V infection arrests CD36^{+} EPCs at a 4 N DNA content but incorporates BrdU. (A and B) Cell cycle analysis of BrdU-pulse-labeled CD36^{+} EPCs. (A) CD36^{+} EPCs were mock infected or infected with B19V. (B) CD36^{+} EPCs were transduced with the lentivirus lenti-p6-NS1, which expresses a codon-optimized NS1, or GFP-expressing lentivirus (shScram) (34) as a control. At the indicated times p.i. or p.t., the cells were incubated with BrdU for 1 h, followed by treatment with 1 N HCl (30). The treated cells were costained with anti-B19V NS1 and anti-BrdU antibodies and DAPI for cell cycle analysis by flow cytometry. The percentage of cells in each phase was gated in the NS1^{+} cell population of the B19V-infected or lenti-P6-NS1-transduced cells, in the GFP[+] cell population of the control lentivirus-transduced cells, and in the whole population of mock-infected cells. In each group, data on both DAPI staining alone (top) and DAPI-BrdU costaining (bottom) are shown. The numbers in the histograms resulting from only DAPI staining are percentages of the cell population at 2 N, intermediate (Int.), and 4 N DNA content, respectively, as indicated. The numbers in each DAPI-BrdU costaining histogram are percentages of the cell populations with all BrdU-positive (BrdU[+]), at a 4 N DNA content with BrdU-positive (BrdU[+]/DNA[4N], in red), and at a 4 N DNA content but with BrdU-negative (BrdU[−]/DNA[4N]) staining, as indicated. (C and D) Statistical analysis. The statistical analyses of the percentages of all the cell populations with BrdU[+] (C) and the cell population with BrdU[+] but only at a 4 N DNA content (BrdU[+]/DNA[4N]) (D), obtained from three independent experiments, are shown. The data are shown as means ± standard deviations. P values were determined using Student's t test.

UT7/Epo-S1 cells with both the wild-type B19V infectious clone (M20) and the M20[mTAD2] mutant.

MATERIALS AND METHODS

Cells and virus. (i) CD36^{+} EPCs. Human bone marrow CD34^{+} hematopoietic stem/progenitor cells (HSCs) were positively isolated using a direct immunomagnetic CD34^{+} MicroBead labeling system and were purchased from AllCells, LLC (Alameda, CA; catalog no. ABM017F). The

CD34^{+} HSCs were *ex vivo* expanded in Wong medium (19, 20). On day 4 of culture, the cells were frozen as stocks. The day 4 HSCs were thawed and cultured in Wong medium under normoxic conditions (21% O_2 and 5% CO_2) until day 7. The day 7 cells were then transferred to hypoxic conditions (1% O_2 and 5% CO_2) for 2 days before infection (22).

(ii) UT7/Epo-S1 cells. UT7/Epo-S1 cells (17) were cultured in Dulbecco's modified Eagle's medium (DMEM) with 10% fetal bovine serum and 2 units/ml of erythropoietin (Epogen; Amgen, Thousand Oaks, CA) at

37°C under normoxic conditions. The cells were kept under hypoxic conditions for 48 h before performing experiments.

(iii) B19V. Viremic plasma sample P265 (~1 × 10^11 genome copies [gc]/ml) was obtained from ViraCor Laboratories (Lee's Summit, MO). Virus infection was performed at a multiplicity of infection (MOI) of 1,000 gc/cell (~3 fluorescence focus-forming units per cell), as described previously (25, 34).

B19V infectious clone and nucleofection. B19V infectious clone pM20 (23), an NS1 endonuclease knockout mutant (pM20^endo−), and an NS1 putative transactivation domain (TAD2) mutant (pM20^mTAD2) were described previously (25). Before nucleofection, the B19V DNA (M20 and its mutants) was excised from the clones by SalI digestion and purified. The SalI-digested backbone DNA was used as a control. All DNAs were nucleofected using an Amaxa nucleofector (Lonza Inc., NJ) as previously described (35).

Lentivirus and transduction. A plenti-p6-B19V-optimized NS1 plasmid (p6-NS1) and p6-NS1-based vectors that express NS1 mutant NS1(mTAD2) and NS1(endo−), respectively, have been described previously (25). pLKO-shRNA-MCM2 (for shMCM2) and pLKO-shRNA-MCM5 (for shMCM5) were made by inserting short hairpin RNA (shRNA) sequences—5′-CCG GGC ACA AGG TAC GTG GTG ATA TCT CGA GAT ATC ACC ACG TAC CTT GTG CTT TTT-3′ and 5′-CCG GGC ACA GCA TCA TCA AGG ACT TCT CGA GAA GTC CTT GAT GAT GCT GTG CTT TTT-3′, respectively—into the pLKO-GFP vector, as described previously (34).

Lentiviruses were produced by transfecting the lentiviral vectors in 293T cells, purified, and transduced as previously described (22, 25).

Western blotting and immunofluorescence. Western blotting and immunofluorescence assays were performed as described previously (34). For immunofluorescence analysis of proliferating cell nuclear antigen (PCNA), the cells were permeabilized with 90% methanol. Confocal images were taken with an Eclipse C1 Plus confocal microscope (Nikon) controlled by Nikon EZ-C1 software.

Southern blot analysis. Low-molecular-weight DNA (Hirt DNA) was extracted from cells as described previously (35, 36). Southern blotting was performed as described previously using the SalI-digested M20 DNA, which contains a full-length B19V genome (34, 35), as a probe.

BrdU-based dot blot assay. CD36^+ EPCs were mock or B19V infected. At 12 h, 24 h, and 48 h postinfection (p.i.), the infected cells were labeled with BrdU (30 μM) for 1 h and collected. Equivalent numbers of cells were used to prepare total DNA and Hirt DNA. Total DNA (both cellular DNA and viral DNA) was extracted using the DNeasy Blood and Tissue Kit (Qiagen). The kit has been optimized for purification of total DNA from virus-infected tissues and had a recovery rate of over 90% for parvoviral DNA (30). The extracted DNA was diluted in 100 μl of deionized H$_2$O. To expose the BrdU epitopes in double-stranded DNA (dsDNA), the DNA samples were heated at 95°C for 5 min and immediately placed on ice. Five microliters of the denatured DNA samples was pipetted onto a nitrocellulose membrane. The DNA dots on the membrane were analyzed by a BrdU-based dot blot assay that we recently established for studying DNA replication in minute virus of canines (MVC) (30).

Comet assay. Comet assay, a single-cell gel electrophoresis assay, was performed following the manufacturer's instructions using a kit purchased from Cell Biolabs, Inc. (San Diego, CA). Briefly, cells were mixed with 1% low-melting-point agarose, and slides were coated with the mixture. The slides were then treated under alkaline conditions, electrophoresed, and stained. The stained slides were visualized under a Nikon Eclipse C1 Plus confocal microscope.

BrdU incorporation assay and flow cytometry. The BrdU incorporation assay was performed following a method that we established for the analysis of MVC infection-induced S phase arrest (30). Briefly, BrdU was added to the cell culture medium at a final concentration of 30 μM and incubated for 1 h. After BrdU incorporation, cells were collected, fixed in 1% paraformaldehyde for 30 min, and permeabilized with 0.05% Triton
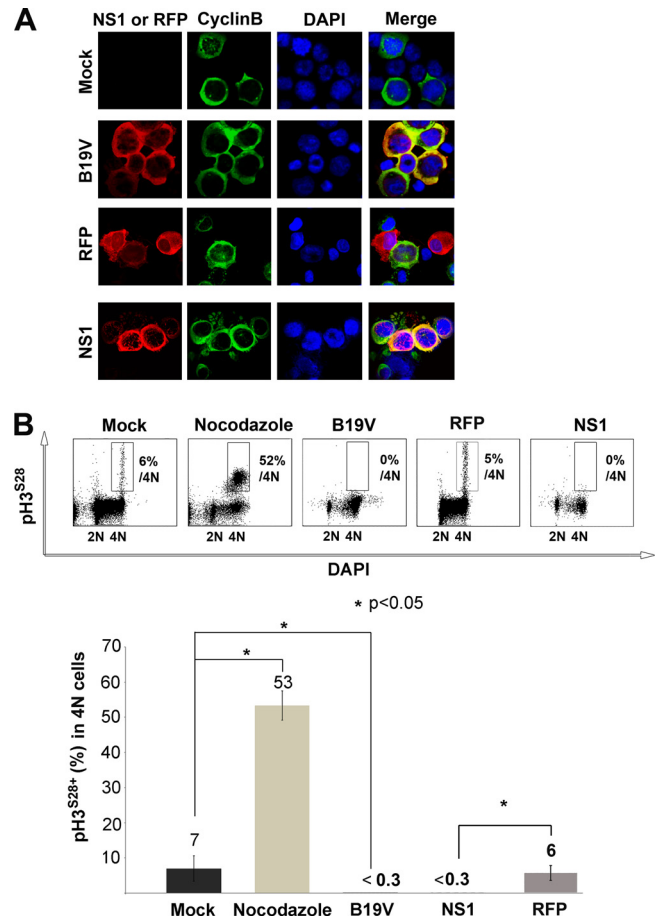

FIG 2 Both B19V infection and lentiviral NS1 transduction block mitosis of CD36^+ EPCs. CD36^+ EPCs were mock infected or infected with B19V or transduced with lenti-p6-NS1 (NS1) or Lenti-½ITR-P6-RFP (RFP) (25). At 48 h p.i./p.t., the cells were analyzed by immunofluorescence assay (A) or flow cytometry (B). (A) Immunofluorescence assay. The cells were fixed and costained with anti-cyclin B and anti-NS1 antibodies and DAPI. Confocal images were taken at a magnification of ×100. (B) Flow cytometry. The cells were fixed and costained with anti-pH 3^S28 and anti-NS1 antibodies and DAPI. NS1^+ cells were selected for flow cytometry analysis (30). Cells treated with nocodazole (at 50 ng/ml) for 16 h were used as a positive control for anti-pH 3^S28 staining. The numbers indicate the percentages of the pH 3^S28-positive cells with a 4 N DNA content in each group. A statistical analysis of the percentages was performed from three independent comet assays. The data are shown as means ± standard deviations.

X-100 for 20 min. After permeabilization, the cells were treated with 1 M HCl for 30 min to denature dsDNA for binding of the BrdU epitopes with an anti-BrdU antibody (clone B44 [37]). The cells were then costained with anti-BrdU and anti-B19V NS1 antibodies, followed by staining of secondary antibodies and DAPI (4′,6-diamidino-2-phenylindole) staining to analyze the cell cycle and NS1-positive (NS^+) cells, respectively.

All the processed samples were analyzed on a three-laser flow cytometer (LSR II; BD Biosciences) at the Flow Cytometry Core. All the flow cytometry data were analyzed using FACS DIVA software (BD Biosciences). Dead cells were excluded by forward scatter (FSC) versus side scatter (SSC) dot plot analysis. Cell cycle analysis was determined by the histogram established based on the DAPI-stained DNA content (DAPI) and the BrdU incorporation (BrdU) detected by an anti-BrdU antibody. Cell cycle gating was based on two separate methods: the mock-infected cell group was used for the B19V-infected cell group and the control lentivirus group for the lentivirus-transduced group. The percentage of
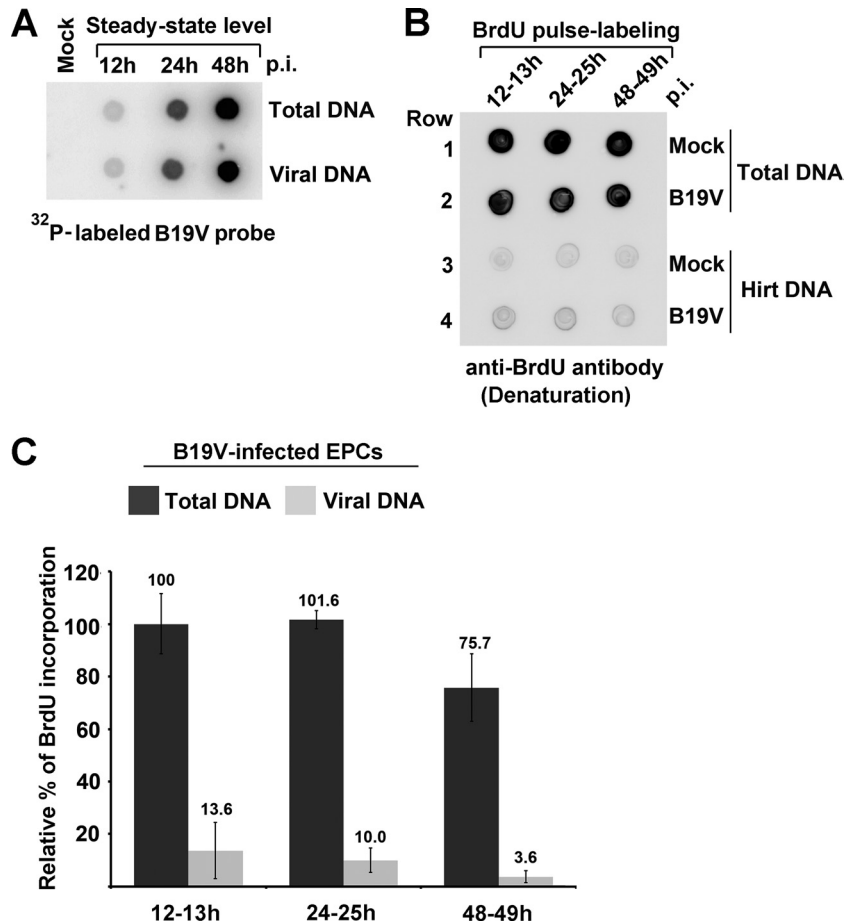
FIG 3 Dot blot analysis of viral and cellular DNA replication. At 12 h, 24 h, and 48 h p.i., mock- or B19V-infected EPCs were incubated with BrdU for 1 h. BrdU-pulse-labeled cells were collected and extracted for total DNA and Hirt DNA (viral DNA). The DNA samples were denatured and pipetted onto a nitrocellulose membrane, followed by UV cross-linking. (A) Dot blot DNA hybridization analysis for the steady-state level of viral DNA. The membrane was hybridized with a ^{32}P-labeled B19V DNA probe. The image was acquired by scanning the hybridized membrane using a Typhoon FLA 9000 phosphorimager. (B and C) BrdU dot blot analysis for transient DNA replication. The membrane was analyzed by a Western blotting procedure with an anti-BrdU antibody. (B) A representative experiment is shown. (C) A statistical analysis of the BrdU content in total DNA and viral DNA of B19V-infected cells was performed from three independent experiments. The BrdU content in the sample prepared at 12 h p.i. from B19V-infected cells was arbitrarily set as 100%. The viral DNA content was calculated by subtracting the BrdU signal in the mock-infected group from the signal of a Hirt DNA sample of B19V-infected cells at the same time p.i.

cells in each phase was gated in the NS1^{+} cell population of the B19V-infected or lenti-p6-NS1-transduced cells, in the GFP^{+} cell population of the control lentivirus-transduced cells, and in the whole population of mock-infected cells.

Antibodies used in the study. Rat anti-B19V NS1 polyclonal antibody (serum) was produced previously (21). Other antibodies obtained commercially include the following: anti-MCM2 and anti-MCM5 (Epitomics, Burlingame, CA); anti-BrdU (clone B44) and anti-PCNA antibodies (BD Biosciences, San Jose, CA); anti-β-actin (Sigma, St. Louis, MO); anti-cyclin A, anti-replication factor C1 (RFC1), and anti-polymerase δ (Pol δ) (Santa Cruz Biotechnology, Santa Cruz, CA); anti-cyclin B (Abcam, Cambridge, MA); and anti-phosphorylated histone 3 at serine 28 (pH 3^{S28}) (Abcam, Cambridge, MA). All the secondary antibodies were purchased from Jackson ImmunoResearch Laboratories, Inc., West Grove, PA. The antibody dilutions used for Western blotting and immunofluorescence analysis were those suggested by the manufacturers.

RESULTS

B19V-infected CD36^{+} EPCs are arrested at a phase with a 4 N DNA content but take up BrdU. We and others have analyzed the cell cycle change of B19V-infected CD36^{+} EPCs by DAPI staining of DNA alone and revealed that infected cells were quickly arrested at a phase with a 4 N DNA content (24, 25). However, a limitation of the DNA-staining method is that it prevents us from differentiating cells at the border of two phases of the cell cycle, e.g., G$_1$ versus early S phase and G$_2$ versus late S phase. Recently, by incorporating BrdU pulse-labeling and flow cytometry, we have precisely analyzed the cell cycle change of MVC-infected cells and identified an intra-S phase arrest during MVC infection (30).

To dissect the 4 N phase arrest of B19V-infected CD36^{+} EPCs, we pulse-labeled infected cells with BrdU and performed cell cycle analysis by flow cytometry using costaining of an anti-BrdU antibody and DAPI. Because of the nature of primary CD36^{+} EPCs, a long processing time, and the harsh conditions of HCl treatment, a large portion of dead cells caused by B19V infection or NS1 transduction became cell debris and were lost during processing. The dead cells were further excluded based on FSC versus SSC dot plot analysis during flow cytometry analysis. In comparison with mock-infected EPCs, B19V infection caused >90% of NS1^{+} EPCs to have a 4 N DNA content as early as 12 h p.i. (Fig. 1A, B19V cell
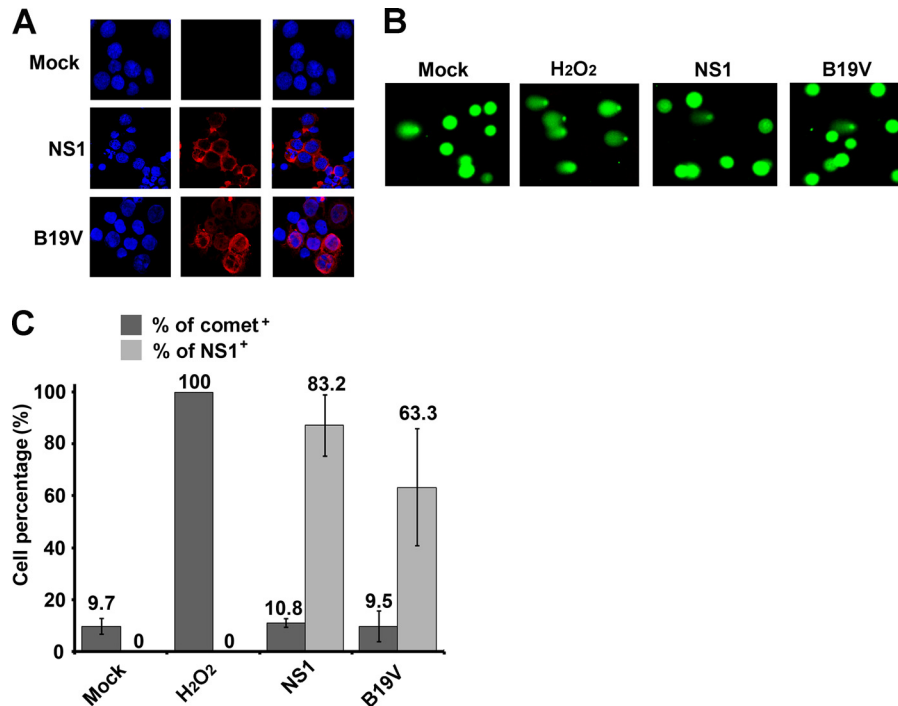
FIG 4 B19V infection does not induce significant cellular DNA damage. CD36$^+$ EPCs were mock infected, infected with B19V, or transduced with the lentivirus lenti-p6-NS1 (NS1). (A) At 18 h p.i., half of the cells were fixed and costained with a rat anti-NS1 antibody and DAPI to quantify the percentage of B19V-infected/lentivirally transduced (NS1$^+$) cells by immunofluorescence assay. Confocal images were taken at a magnification of ×40 (objective lens). (B) The other half of the cells were collected and analyzed for damaged DNA (Comet$^+$) using a comet assay kit. Positive controls (H$_2$O$_2$) were obtained by treating mock-infected cells with 100 μM H$_2$O$_2$ at 4°C for 20 min. The images were taken at a magnification of ×40. (C) A statistical analysis of the percentage of cells with damaged DNA was performed from three independent comet assays. In each experiment, cells were counted on six randomly selected fields with ~100 to 200 cells each. The data are shown as means ± standard deviations.

count), which is consistent with our previous report (25). We observed this phenomenon as soon as NS1 became detectable (at 8 h p.i.) (data not shown) and did not observe a progression process (Fig. 1A, B19V cell count). Notably, when a BrdU incorporation assay was performed, ~40 to 50% of the NS1$^+$ cells were anti-BrdU positive (BrdU$^+$) as early as 12 h p.i., which continued to late infection (at 48 h p.i.), whereas only ~25% of mock-infected cells were BrdU$^+$ (Fig. 1A, BrdU$^+$, and C, B19V). Further analysis of the BrdU$^+$ population showed that ~30 to 50% of the NS1$^+$ cells actually had a 4 N DNA content compared with only ~10% of the mock-infected cells (Fig. 1A, BrdU$^+$/DNA^{4N}, and D, B19V). This result suggested that a large portion of NS1$^+$ cells that had a 4 N DNA content still incorporated BrdU.

To assess whether B19V NS1 expression mimics the cell cycle change during infection, we transduced CD36$^+$ EPCs with an NS1-expressing lentivirus (Lenti-p6-NS1) (25). Over 90% of the NS1$^+$ cells were arrested at a 4 N DNA content (Fig. 1B, NS1 cell count), and an average of over 79% of the NS1$^+$ cells were arrested at G$_2$/M phase (BrdU$^-$/DNA^{4N}), during the course of transduction (Fig. 1B, NS1/BrdU). This result confirmed that B19V NS1 arrests NS1-lentivirus-transduced cells at G$_2$/M phase (BrdU$^-$/DNA^{4N}). However, compared to 25.5% of the control-transduced cells, only 13.2% of the NS1$^+$ cells were able to incorporate BrdU at 12 h postransduction (p.t.), and this number decreased significantly with time (Fig. 1C, NS1), indicating that cellular DNA replication was gradually blocked in these cells. Notably, no increase in the cell population at late S phase (BrdU$^+$/DNA^{4N}) was observed (Fig. 1B, BrdU$^+$/DNA^{4N}, and D, NS1).

In addition, we also observed that a small portion of NS1-transduced cells stayed at G$_1$ phase (10.7%, 13.8%, and 16.9% at 12, 24, and 48 h p.i., respectively) (Fig. 1B, BrdU). However, the portion of infected cells at G$_1$ phase was even smaller in B19V-infected EPCs (4.9%, 3.8%, and 5.4% at 12, 24, and 48 h p.i., respectively) (Fig. 1A, BrdU).

To determine whether B19V-infected and NS1-transduced CD36$^+$ EPCs enter mitosis, we performed immunofluorescence analysis for cyclin B, a mitotic cyclin that is shuttled to the nucleus when it triggers mitosis entry (38). We found that cyclin B was trapped in the cytoplasm of either B19V-infected or NS1-transduced cells, compared with the cyclin B in control cells (Fig. 2A), suggesting that both infected and transduced cells are arrested at G$_2$ or a "pseudo-G$_2$" phase. In concert, pH 3^{S28}, a marker of mitosis (39), was totally gone in both B19V-infected and NS1-transduced cells compared with the pH 3^{S28} in control cells (Fig. 2B), confirming that the cells were not able to enter mitosis.

Taken together, our results suggest that B19V-infected CD36$^+$ EPCs have a 4 N DNA content, still incorporate BrdU, and are arrested at a phase with an increase in cytoplasmic cyclin B and an absence of phosphorylated histone 3 (BrdU$^+$/DNA^{4N}/cyclin B$^+$/pH 3^{S28-}), whereas B19V NS1 expression mainly arrests cells at a bona fide G$_2$ phase (BrdU$^-$/DNA^{4N}/cyclin B$^+$/pH 3^{S28-}) without BrdU incorporation.

Viral DNA replication contributes minimally to BrdU incorporation. BrdU incorporation could be contributed by several sources: (i) viral DNA replication, (ii) DNA repair-associated DNA synthesis, and (iii) cellular DNA replication in S phase. In
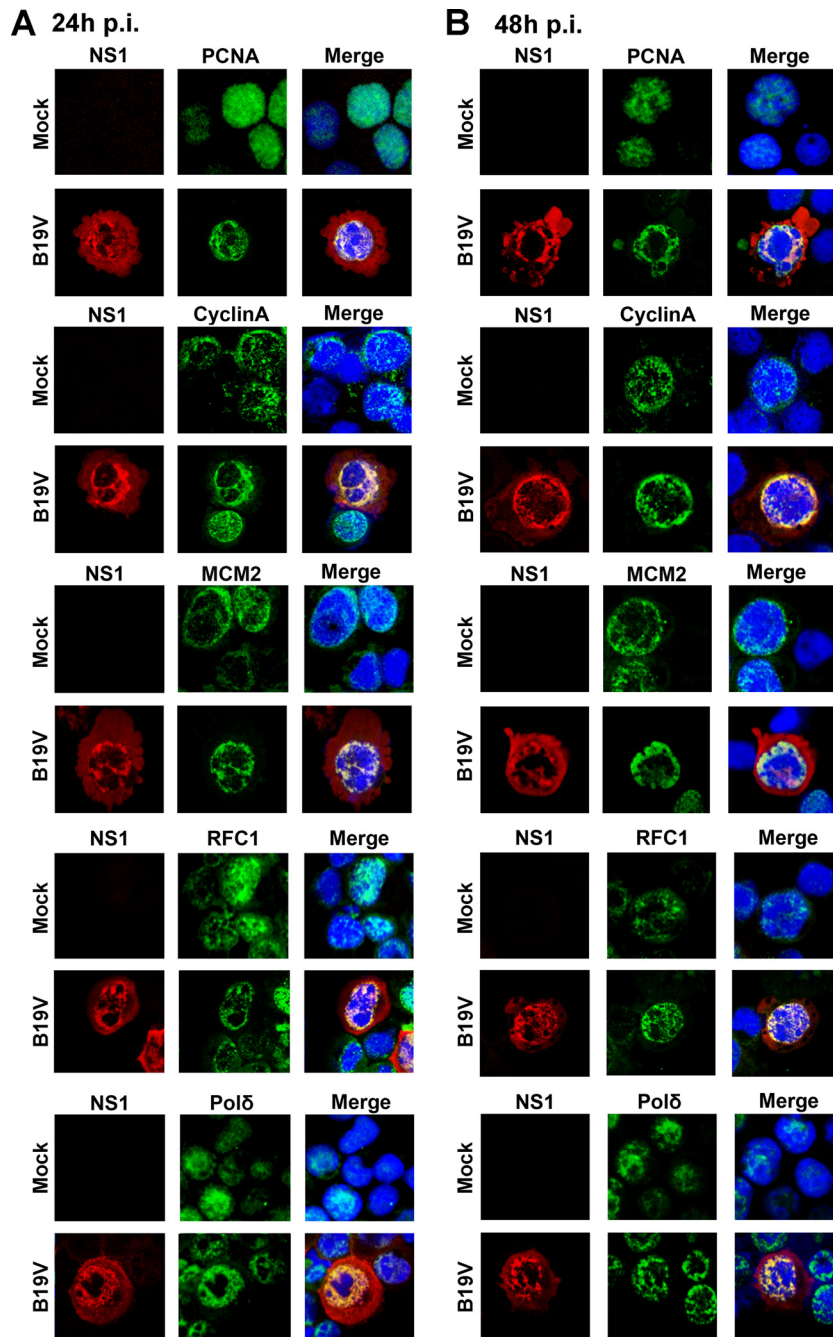
FIG 5 Immunofluorescence staining of cellular S phase factors. At 24 h p.i. (A) and 48 h p.i. (B), mock- and B19V-infected CD36$^+$ EPCs were fixed and costained with anti-B19V NS1 and an antibody against one of the S phase factors, as indicated, and DAPI. The images were taken at a magnification of ×100.

our previous study, we confirmed that DNA replication of the parvovirus MVC does not contribute significantly to BrdU uptake in the BrdU incorporation assay (30). To ensure this was true during B19V infection of CD36$^+$ EPCs, we extracted total DNA and low-molecular-weight (Hirt) DNA from BrdU-labeled infected cells and examined the BrdU uptake in each sample using a BrdU dot blot assay, as we described previously (30). As shown in Fig. 3A, the amount of viral DNA extracted by the Hirt DNA preparation method was nearly the same as that extracted by the total-DNA preparation method. However, the Hirt DNA prepa-

ration method was not able to eliminate all cellular DNA, as the mock-infected group also had some weak signals (Fig. 3B, row 3). Thus, the BrdU incorporation in Hirt DNA samples contained both viral DNA and a small amount of cellular DNA (Fig. 3A, row 4). The BrdU incorporation in viral DNA was quantified by subtracting the background BrdU signal, which appeared in the Hirt DNA of the mock-infected group (Fig. 3B, row 3), from the signal of the Hirt DNA of the B19V-infected group (Fig. 3A, row 4) at the same time p.i. The quantification data showed that the BrdU incorporation in viral DNA was only 13.6% of the BrdU signal in

total DNA at 12 h p.i. and was much lower at 24 h and 48 h p.i. (Fig. 3C). These results confirmed that the majority of BrdU is actually incorporated in cellular DNA.

Collectively, our results presented so far indicated that the BrdU incorporation in B19V-infected cells, which are arrested at a phase with a 4 N DNA content, comes from cellular DNA synthesis triggered by DNA repair or from cellular DNA replication in late S phase.

B19V infection does not induce significant cellular DNA damage. B19V infection induces a DNA damage response (DDR) (25, 34). We wondered whether cellular DNA damage is caused during B19V infection, which could be followed by cellular DNA repair events (40). To determine whether the BrdU uptake in B19V-infected CD36$^+$ EPCs is due to cellular DNA repair, we performed a comet assay (41, 42), as we described previously (30), to assess if there is any cellular DNA damage in B19V-infected CD36$^+$ EPCs. At 48 h p.i./p.t., ~60% and ~80% of CD36$^+$ EPCs, respectively, as shown by anti-NS1 staining, were infected with B19V or transduced by lenti-p6-NS1 (Fig. 4A); however, the population of comet-positive (Comet$^+$) cells (~10%) in infected or transfected cells was not significantly increased compared with that in the mock-infected cells (Fig. 4B and C). This result confirmed that B19V infection does not induce severe cellular DNA damage, suggesting that the BrdU incorporation in B19V-infected CD36$^+$ EPCs likely does not come from cellular DNA repair.

Together with the aforementioned evidence that B19V DNA replication does not contribute significantly to BrdU incorporation in B19V-infected EPCs (Fig. 3), our results strongly suggested that B19V infection mainly induces cells arrested at late S phase (BrdU$^+$/DNA^{4N}/cyclin B$^+$/pH 3^{S28-}) during early infection.

Cellular DNA replication factors colocalize with B19V NS1 in B19V DNA replication centers. To confirm the S phase status of B19V-infected CD36$^+$ EPCs, we examined the localization of five S phase (DNA replication) factors, i.e., cyclin A, PCNA, RFC1, MCM2, and Pol δ, since they have been reported to play roles in parvovirus DNA replication (29, 43–45). We found that these five S phase factors were abundantly expressed in NS1$^+$ CD36$^+$ EPCs and colocalized with the foci stained for B19V NS1, which are the B19V replication centers (34), over the course of infection (Fig. 5). We then attempted to knock down the S phase factors to explore their roles in B19V DNA replication. Since they are required for cell proliferation, we chose the abundantly expressed MCM2/MCM5 for this purpose. The MCM complex is thought to be the major DNA helicase that is abundantly and redundantly expressed for eukaryotic-cell DNA replication (46). Indeed, individual knockdown of 50% of MCM2 or MCM5 did not obviously change the cell cycle pattern compared to control-transduced CD36$^+$ EPCs (Fig. 6A and B, shScram.); however, the major species of B19V replicated DNA (replicative-form [RF] DNA) decreased >3-fold in either MCM2 shRNA (shMCM2)- or MCM5 shRNA (shMCM5)-treated EPCs compared with those in scrambled shRNA (shScram)-treated EPCs (Fig. 6C). This result suggested that B19V DNA replication was significantly inhibited by knockdown of MCM2 or MCM5 in infected EPCs.

Collectively, these results demonstrated that although B19V-infected EPCs were arrested at a 4 N DNA content and had cytoplasmically accumulated cyclin B, S phase factors were expressed and colocalized within the B19V replication centers in the nuclei, which likely facilitate B19V DNA replication.

A mutant B19V infectious DNA that abolishes cell cycle arrest at a 4 N DNA content induces S phase arrest in transfected UT7/Epo-S1 cells. To examine specifically the cell cycle status of
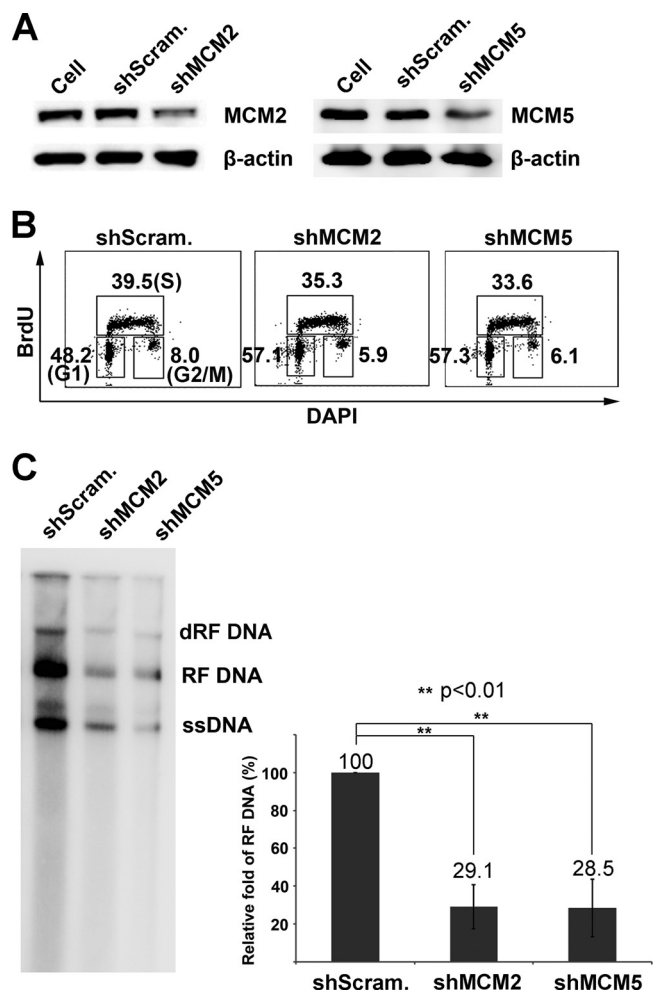

FIG 6 Cell cycle analysis of MCM2 and MCM5 knockdown CD36$^+$ EPCs. CD36$^+$ EPCs were transduced with the indicated shRNAs for 48 h. (A) Western blotting. Cells were harvested and analyzed by Western blotting with anti-β-actin and anti-MCM2 or anti-MCM5. (B) Flow cytometry analysis. Cells were analyzed by BrdU incorporation assay for cell cycle patterns. The numbers are the percentages of the cells in G$_1$, S, and G$_2$/M phases, as indicated. (C) Southern blot analysis of B19V DNA replication. CD36$^+$ EPCs were transduced with the indicated shRNAs and infected with B19V for 48 h. Hirt DNA samples were prepared and analyzed by Southern blotting. The blots were exposed to a phosphorimaging screen, and the RF DNA was quantified using a Typhoon FLA 9000 phosphorimager and ImageQuant TL (version 4.2.2) imaging software (GE Healthcare). A statistical analysis of the relative percentage of the RF DNA was performed from three independent experiments. The intensity of the RF DNA isolated in shScram-treated cells was arbitrarily set as 100%. dRF DNA, double-RF DNA; ssDNA, single-stranded DNA.

the cells that facilitate B19V DNA replication, we took advantage of the DNA replication of the B19V infectious DNA (M20) in UT7/Epo-S1 cells cultured under hypoxic conditions (22, 25). We have identified a B19V mutant infectious DNA, M20^{mTAD2}, that replicates efficiently in UT7/Epo-S1 cells but without significantly arresting the cells at a 4 N DNA content (25). To determine precisely the cell cycle change during the replication of this mutant, we transfected the wild-type M20 DNA and its mutants, M20^{mTAD2} and M20^{endo-} (a nonreplicative mutant as a negative control [25]), into UT7/Epo-S1 cells and performed a BrdU incorporation assay at 48 h posttransfection. We found that M20
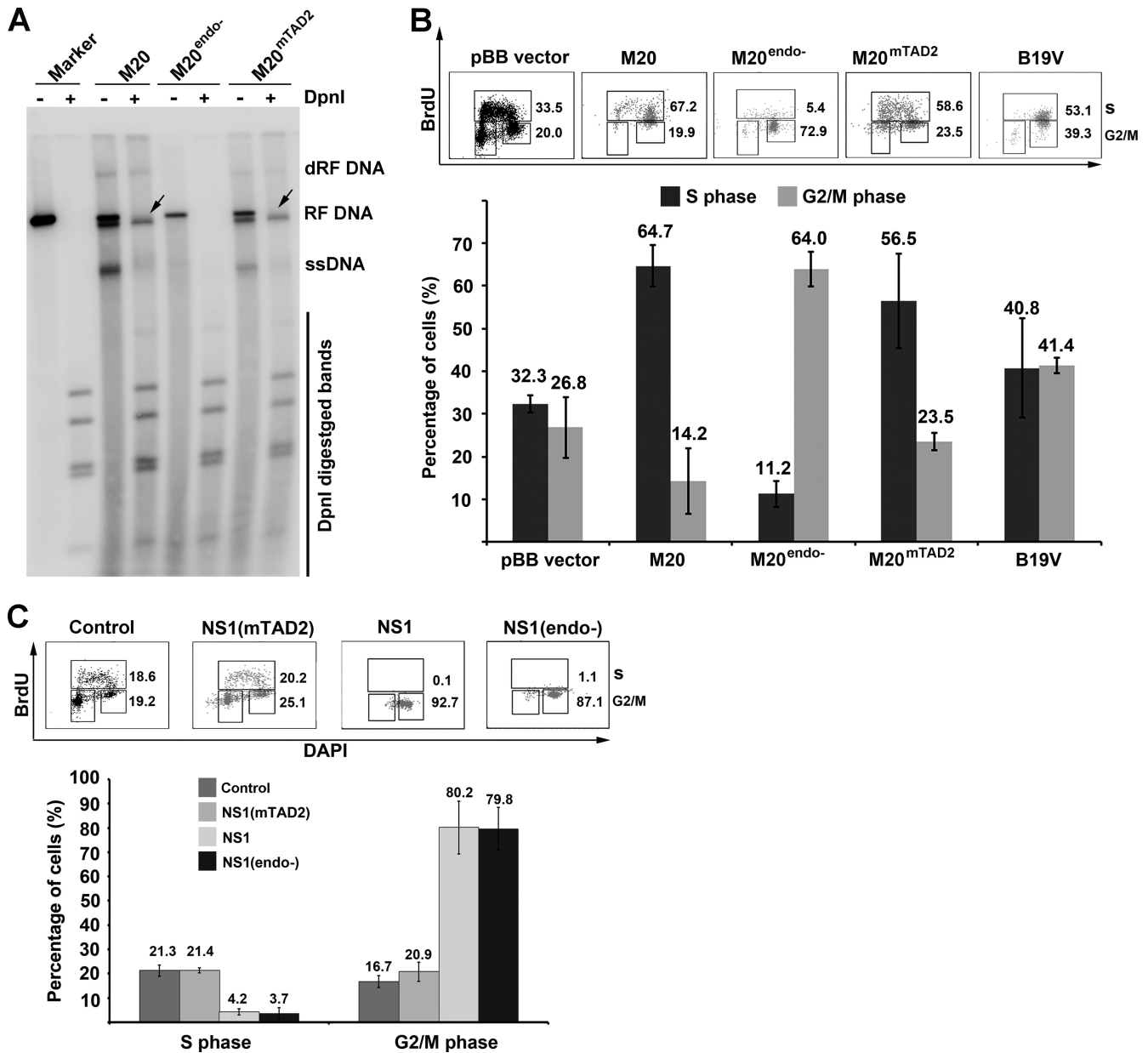
FIG 7 B19V infectious DNAs M20 and M20^{mTAD2} replicate in UT7/Epo-S1 cells at S phase. (A and B) Wild-type B19V infectious DNA M20, the endonuclease knockout mutant M20^{endo-} DNA, and the mTAD2 mutant M20^{mTAD2} DNA were transfected into UT7/Epo-S1 cells. (A) Southern blot analysis of B19V DNA replication. At 48 h posttransfection, cells were collected and prepared for Hirt DNA samples. The samples were digested with (+) or without (−) DpnI and subjected to Southern blotting. The arrows indicate DpnI-resistant bands. (B) Cell cycle analysis of M20-based B19V DNA-transfected cells. At 48 h posttransfection, the cells were labeled with BrdU. (C) Cell cycle analysis of cells transduced with NS1-expressing lentiviruses. UT7/Epo-S1 cells were transduced with either the lentivirus lenti-p6-NS1, which expresses wild-type NS1 (NS1), or lenti-p6-NS1-based lentiviruses that express NS1 mutant NS1(mTAD2) and NS1(endo−), respectively, and a GFP-expressing control lentivirus (Control). At 48 h p.t., the cells were labeled with BrdU for 1 h. NS1^{+} (or GFP^{+}) cells were selected for cell cycle analysis by flow cytometry. The numbers are cell populations in S phase (BrdU^{+}) and G$_2$/M phase (BrdU$^{−}$/DNA^{4N}), as indicated. B19V infection of UT7/Epo-S1 cells was used as a control. A statistical analysis of the percentage of cells at each phase was performed from three independent experiments. The data are shown as means ± standard deviations.

and M20^{mTAD2} replicated in UT7/Epo-S1 cells at similar levels, as evidenced by the DpnI digestion-resistant bands (Fig. 7A, arrows). As we previously reported (47), electroporation and NS1/11-kDa expression caused significant death of UT7/Epo-S1 cells. Dead cells appearing as cell debris were lost during the staining procedure and further excluded by FSC versus SSC dot plot analysis in flow cytometry, which allowed us to analyze the cell cycle of the

live cells by the BrdU incorporation assay. The results showed that 64.7% and 64.0% of the NS1^{+} cells in M20- and M20^{mTAD2}-transfected cells, respectively, were arrested at S phase (BrdU^{+}) compared with 32.3% of the control cells (Fig. 7B). Notably, M20-transfected cells were arrested more at late S phase (>80% of the BrdU^{+} cells at DNA^{4N}), while M20^{mTAD2} transfection arrested cells at early S phase (>65% of the BrdU^{+} cells at DNA^{2N})

(Fig. 7B). In contrast, the majority of M20^{endo-}-transfected (NS1$^+$) cells (64.0%) were arrested at G$_2$/M phase (BrdU$^-$/DNA^{4N}).

Notably, only expression of B19V NS1, either the wild type (NS1) or the NS1 mutants NS1(endo−) and NS1(mTAD2), did not arrest UT7/Epo-S1 cells at S phase (BrdU$^+$) (Fig. 7C). Taken together, these results demonstrated that B19V DNA replication that involves NS1, rather than NS1 expression *per se*, is necessary for B19V replication-induced S phase arrest.

DISCUSSION

Modulation of the cell cycle pattern is an important strategy for DNA virus replication. In this study, we have demonstrated for the first time, that B19V infection of CD36$^+$ EPCs induces late S phase arrest (BrdU$^+$/DNA^{4N}/cyclin B$^+$/pH 3^{S28-}), rather than 4 N (G2/M) phase arrest, as previously thought, during early infection. Our results also suggest that the cellular S phase environment is required for efficient B19V DNA replication, which is consistent with the S phase-dependent parvoviral DNA replication (26–32).

We have previously demonstrated that B19V DNA replication induces a DDR that activates ATR/Chk1 signaling (25, 34). ATR/Chk1 activation is known to be able to induce intra-S phase arrest (48). It is likely that B19V DNA replication-induced DDR is involved in the induction of S phase arrest. In parvovirus MVC infection, virus infection-induced DDR activates ATM-SMC1 signaling, which arrests infected cells at the intra-S phase (30). We speculate that there is a feedback loop during autonomous parvovirus replication: viral DNA replication induces a DDR; the DDR activates ATM or ATR signaling, which arrests the cells at S phase; and the S phase environment, in turn, facilitates virus DNA replication.

In addition to the 4 N phase arrest, B19V NS1 also induced G$_1$ phase arrest of infected UT7/Epo-S1 cells (10.9% at G$_1$ versus 81.5% at G$_2$), and this G$_1$ arrest is more significant in NS1-transfected cells (24.5% versus 32.8%) (16). The G$_1$ checkpoint has also been observed in replication of other parvoviruses (26, 49, 50). In CD36$^+$ EPCs, however, fewer NS1$^+$ cells stayed at G$_1$ phase during infection and NS1-lentiviral transduction (4.9 to 5.4% and 10.7 to 16.9%, respectively). The cells that stayed at G$_1$ phase are either the NS1$^+$ cells that exited from mitosis or the NS1$^+$ cells arrested at G$_1$. Since NS1$^+$ cells did not enter mitosis, as indicated by anti-pH 3^{S28} staining (Fig. 2B), we conclude that NS1 also induces a minor G$_1$ arrest in CD36$^+$ EPCs.

A clear progression of G$_1$ to early and late S phase was not observed at early infection (Fig. 1) and in previous studies (17, 24, 25). It is possible that during B19V infection, infected cells are arrested at S phase by the DDR, which is presumably induced by the invaded aberrant viral genome (51) and a low level of viral DNA replication before expression (detection) of NS1 at early infection. On the other hand, expression of NS1 tends to push the cells abruptly into G$_2$ phase but is not able to complete this step during early infection. The incomplete G$_2$ phase arrest, i.e., late S phase arrest, still allows a low level of cellular DNA replication to reserve S phase factors for facilitating viral genome amplification. This theory can explain why the M20^{mTAD2} mutant, which loses the capability to induce G$_2$ phase arrest, replicates in UT7-Epo/S1 cells during the entire S phase (BrdU$^+$).

B19V NS1, a multifunctional protein during virus replication (52, 53), also induces G$_2$/M arrest (Fig. 1B) (16, 24, 25) and apoptosis (18, 47, 54, 55). The G$_2$ phase arrest has been shown to be induced by deregulation of the E2F4/E2F5 transcription factors (24). However, the mechanism underlying NS1-induced apoptosis is largely unknown (56). It is possible that NS1-induced G$_2$ arrest is one of the functions through which NS1 inhibits erythropoiesis and kills infected erythroid progenitors for progeny virion release, whereas the late S phase arrest is a compromised transition situation resulting from the G$_2$ phase arrest by NS1 and the intra-S phase arrest caused by the DDR. On the other hand, MVC NS1 *per se* does not induce G$_2$ phase arrest and apoptosis (57), and therefore, MVC infection appears only during the intra-S phase arrest (30).

In summary, parvovirus has a compact genome that does not express a viral protein specifically to manipulate the S phase of the cell cycle. Except for the Rep78 protein of *Dependoparvovirus* AAV (58), the large nonstructural proteins of autonomous parvoviruses do not arrest cells in S phase. Thus, autonomous parvoviruses evolve to find a way through DDR to arrest cells in S phase that facilitates viral DNA replication. It is clear now that B19V also uses this approach to take advantage of the S phase factors for viral DNA replication. Finally, we demonstrated that expression of NS1 *per se* is responsible for the true G$_2$/M (4 N/BrdU$^-$) phase arrest.

ACKNOWLEDGMENTS

REFERENCES

1. **Weir E.** 2005. Parvovirus B19 infection: fifth disease and more. CMAJ **172:**743.
2. **Young NS, Brown KE.** 2004. Parvovirus B19. N. Engl. J. Med. **350:**586–597.
3. **Lamont R, Sobel J, Vaisbuch E, Kusanovic J, Mazaki-Tovi S, Kim S, Uldbjerg N, Romero R.** 2011. Parvovirus B19 infection in human pregnancy. BJOG **118:**175–186.
4. **Riipinen A, Vaisanen E, Nuutila M, Sallmen M, Karikoski R, Lindbohm ML, Hedman K, Taskinen H, Soderlund-Venermo M.** 2008. Parvovirus B19 infection in fetal deaths. Clin. Infect. Dis. **47:**1519–1525.
5. **Anderson MJ, Khousam MN, Maxwell DJ, Gould SJ, Happerfield LC, Smith WJ.** 1988. Human parvovirus B19 and hydrops fetalis. Lancet **i:**535.
6. **Tavil B, Sanal O, Turul T, Yel L, Gurgey A, Gumruk F.** 2009. Parvovirus B19-induced persistent pure red cell aplasia in a child with T-cell immunodeficiency. Pediatr. Hematol. Oncol. **26:**63–68.
7. **Mrzljak A, Kardum-Skelin I, Cvrlje VC, Kanizaj TF, Sustercic D, Gustin D, Kocman B.** 2010. Parvovirus B 19 (PVB19) induced pure red cell aplasia (PRCA) in immunocompromised patient after liver transplantation. Coll. Antropol. **34:**271–274.
8. **Shade RO, Blundell MC, Cotmore SF, Tattersall P, Astell CR.** 1986. Nucleotide sequence and genome organization of human parvovirus B19 isolated from the serum of a child during aplastic crisis. J. Virol. **58:**921–936.
9. **Duncan JR, Potter CB, Cappellini MD, Kurtz JB, Anderson MJ, Weatherall DJ.** 1983. Aplastic crisis due to parvovirus infection in pyruvate kinase deficiency. Lancet **ii:**14–16.
10. **Rechavi G, Vonsover A, Manor Y, Mileguir F, Shpilberg O, Kende G, Brok-Simoni F, Mandel M, Gotlieb-Stematski T, Ben-Bassat I.** 1989. Aplastic crisis due to human B19 parvovirus infection in red cell pyrimidine-5′-nucleotidase deficiency. Acta Haematol. **82:**46–49.
11. **Cotmore SF, Tattersall P.** 1984. Characterization and molecular cloning of a human parvovirus genome. Science **226:**1161–1165.
12. **Ozawa K, Ayub J, Hao YS, Kurtzman G, Shimada T, Young N.** 1987. Novel transcription map for the B19 (human) pathogenic parvovirus. J. Virol. **61:**2395–2406.
13. **Ozawa K, Kurtzman G, Young N.** 1986. Replication of the B19 parvovirus in human bone marrow cell cultures. Science **233:**883–886.

14. **Srivastava A, Lu L.** 1988. Replication of B19 parvovirus in highly enriched hematopoietic progenitor cells from normal human bone marrow. J. Virol. **62**:3059–3063.

15. **Morey AL, Fleming KA.** 1992. Immunophenotyping of fetal haemopoietic cells permissive for human parvovirus B19 replication in vitro. Br. J. Haematol. **82**:302–309.

16. **Morita E, Nakashima A, Asao H, Sato H, Sugamura K.** 2003. Human parvovirus B19 nonstructural protein (NS1) induces cell cycle arrest at G(1) phase. J. Virol. **77**:2915–2921.

17. **Morita E, Tada K, Chisaka H, Asao H, Sato H, Yaegashi N, Sugamura K.** 2001. Human parvovirus B19 induces cell cycle arrest at G(2) phase with accumulation of mitotic cyclins. J. Virol. **75**:7555–7563.

18. **Sol N, Le JJ, Vassias I, Freyssinier JM, Thomas A, Prigent AF, Rudkin BB, Fichelson S, Morinet F.** 1999. Possible interactions between the NS-1 protein and tumor necrosis factor alpha pathways in erythroid cell apoptosis induced by human parvovirus B19. J. Virol. **73**:8762–8770.

19. **Wong S, Zhi N, Filippone C, Keyvanfar K, Kajigaya S, Brown KE, Young NS.** 2008. Ex vivo-generated CD36+ erythroid progenitors are highly permissive to human parvovirus B19 replication. J. Virol. **82**:2470–2476.

20. **Chen AY, Guan W, Lou S, Liu Z, Kleiboeker S, Qiu J.** 2010. Role of erythropoietin receptor signaling in parvovirus B19 replication in human erythroid progenitor cells. J. Virol. **84**:12385–12396.

21. **Guan W, Wong S, Zhi N, Qiu J.** 2009. The genome of human parvovirus B19 virus can replicate in non-permissive cells with the help of adenovirus genes and produces infectious virus. J. Virol. **83**:9541–9553.

22. **Chen AY, Kleiboeker S, Qiu J.** 2011. Productive parvovirus B19 infection of primary human erythroid progenitor cells at hypoxia is regulated by STAT5A and MEK signaling but not HIF alpha. PLoS Pathog. **7**:e1002088. doi:10.1371/journal.ppat.1002088.

23. **Zhi N, Zadori Z, Brown KE, Tijssen P.** 2004. Construction and sequencing of an infectious clone of the human parvovirus B19. Virology **318**:142–152.

24. **Wan Z, Zhi N, Wong S, Keyvanfar K, Liu D, Raghavachari N, Munson PJ, Su S, Malide D, Kajigaya S, Young NS.** 2010. Human parvovirus B19 causes cell cycle arrest of human erythroid progenitors via deregulation of the E2F family of transcription factors. J. Clin. Invest. **120**:3530–3544.

25. **Lou S, Luo Y, Cheng F, Huang Q, Shen W, Kleiboeker S, Tisdale JF, Liu Z, Qiu J.** 2012. Human parvovirus B19 DNA replication induces a DNA damage response that is dispensable for cell cycle arrest at G2/M phase. J. Virol. **86**:10748–10758.

26. **Oleksiewicz MB, Alexandersen S.** 1997. S-phase-dependent cell cycle disturbances caused by Aleutian mink disease parvovirus. J. Virol. **71**:1386–1396.

27. **Deleu L, Pujol A, Faisst S, Rommelaere J.** 1999. Activation of promoter P4 of the autonomous parvovirus minute virus of mice at early S phase is required for productive infection. J. Virol. **73**:3877–3885.

28. **Wolter S, Richards R, Armentrout RW.** 1980. Cell cycle-dependent replication of the DNA of minute virus of mice, a parvovirus. Biochim. Biophys. Acta **607**:420–431.

29. **Bashir T, Horlein R, Rommelaere J, Willwand K.** 2000. Cyclin A activates the DNA polymerase delta-dependent elongation machinery in vitro: a parvovirus DNA replication model. Proc. Natl. Acad. Sci. U. S. A. **97**:5522–5527.

30. **Luo Y, Deng X, Cheng F, Li Y, Qiu J.** 2013. SMC1-mediated intra-S phase arrest facilitates Bocavirus DNA replication. J. Virol. **87**:4017–4032.

31. **Cotmore SF, Tattersall P.** 1987. The autonomously replicating parvoviruses of vertebrates. Adv. Virus Res. **33**:91–174.

32. **Cotmore SF, Tattersall P.** 2005. A rolling-hairpin strategy: basic mechanisms of DNA replication in the parvoviruses, p 171–181. *In* Kerr J, Cotmore SF, Bloom ME, Linden RM, Parrish CR (ed), Parvoviruses. Hoddler Arond, London, United Kingdom.

33. **Davy C, Doorbar J.** 2007. G2/M cell cycle arrest in the life cycle of viruses. Virology **368**:219–226.

34. **Luo Y, Lou S, Deng X, Liu Z, Li Y, Kleiboeker S, Qiu J.** 2011. Parvovirus B19 infection of human primary erythroid progenitor cells triggers ATR-Chk1 signaling, which promotes B19 virus replication. J. Virol. **85**:8046–8055.

35. **Guan W, Cheng F, Yoto Y, Kleiboeker S, Wong S, Zhi N, Pintel DJ, Qiu J.** 2008. Block to the production of full-length B19 virus transcripts by

36. internal polyadenylation is overcome by replication of the viral genome. J. Virol. **82**:9951–9963.

37. **Hirt B.** 1967. Selective extraction of polyoma DNA from infected mouse cell cultures. J. Mol. Biol. **26**:365–369.

38. **Gratzner HG.** 1982. Monoclonal antibody to 5-bromo- and 5-iododeoxyuridine: a new reagent for detection of DNA replication. Science **218**:474–475.

39. **Lindqvist A, Rodriguez-Bravo V, Medema RH.** 2009. The decision to enter mitosis: feedback and redundancy in the mitotic entry network. J. Cell Biol. **185**:193–202.

40. **Goto H, Tomono Y, Ajiro K, Kosako H, Fujita M, Sakurai M, Okawa K, Iwamatsu A, Okigaki T, Takahashi T, Inagaki M.** 1999. Identification of a novel phosphorylation site on histone H3 coupled with mitotic chromosome condensation. J. Biol. Chem. **274**:25543–25549.

41. **Weitzman MD, Lilley CE, Chaurushiya MS.** 2010. Genomes in conflict: maintaining genome integrity during virus infection. Annu. Rev. Microbiol. **64**:61–81.

42. **Olive PL.** 2002. The comet assay. An overview of techniques. Methods Mol. Biol. **203**:179–194.

43. **Shaposhnikov SA, Salenko VB, Brunborg G, Nygren J, Collins AR.** 2008. Single-cell gel electrophoresis (the comet assay): loops or fragments? Electrophoresis **29**:3005–3012.

44. **Bashir T, Rommelaere J, Cziepluch C.** 2001. In vivo accumulation of cyclin A and cellular replication factors in autonomous parvovirus minute virus of mice-associated replication bodies. J. Virol. **75**:4394–4398.

45. **Christensen J, Tattersall P.** 2002. Parvovirus initiator protein NS1 and RPA coordinate replication fork progression in a reconstituted DNA replication system. J. Virol. **76**:6518–6531.

46. **Nash K, Chen W, Muzyczka N.** 2008. Complete in vitro reconstitution of adeno-associated virus DNA replication requires the minichromosome maintenance complex proteins. J. Virol. **82**:1458–1464.

47. **Pacek M, Walter JC.** 2004. A requirement for MCM7 and Cdc45 in chromosome unwinding during eukaryotic DNA replication. EMBO J. **23**:3667–3676.

48. **Chen AY, Zhang EY, Guan W, Cheng F, Kleiboeker S, Yankee TM, Qiu J.** 2010. The small 11kDa non-structural protein of human parvovirus B19 plays a key role in inducing apoptosis during B19 virus infection of primary erythroid progenitor cells. Blood **115**:1070–1080.

49. **Bartek J, Lukas C, Lukas J.** 2004. Checking on DNA damage in S phase. Nat. Rev. Mol. Cell Biol. **5**:792–804.

50. **Hermanns J, Schulze A, Jansen D, Kleinschmidt JA, Schmidt R, zur Hausen H.** 1997. Infection of primary cells by adeno-associated virus type 2 results in a modulation of cell cycle-regulating proteins. J. Virol. **71**:6020–6027.

51. **Op De Beeck A, Sobczak-Thepot J, Sirma H, Bourgain F, Brechot C, Caillet-Fauquet P.** 2001. NS1- and minute virus of mice-induced cell cycle arrest: involvement of p53 and p21(cip1). J. Virol. **75**:11071–11078.

52. **Luo Y, Qiu J.** 2013. Parvovirus infection induced DNA damage response. Future Virol. **8**:245–257.

53. **Zhi N, Mills IP, Lu J, Wong S, Filippone C, Brown KE.** 2006. Molecular and functional analyses of a human parvovirus B19 infectious clone demonstrates essential roles for NS1, VP1, and the 11-kilodalton protein in virus replication and infectivity. J. Virol. **80**:5941–5950.

54. **Gareus R, Gigler A, Hemauer A, Leruez-Ville M, Morinet F, Wolf H, Modrow S.** 1998. Characterization of cis-acting and NS1 protein-responsive elements in the p6 promoter of parvovirus B19. J. Virol. **72**:609–616.

55. **Ozawa K, Ayub J, Kajigaya S, Shimada T, Young N.** 1988. The gene encoding the nonstructural protein of B19 (human) parvovirus may be lethal in transfected cells. J. Virol. **62**:2884–2889.

56. **Moffatt S, Yaegashi N, Tada K, Tanaka N, Sugamura K.** 1998. Human parvovirus B19 nonstructural (NS1) protein induces apoptosis in erythroid lineage cells. J. Virol. **72**:3018–3028.

57. **Chen AY, Qiu J.** 2010. Parvovirus infection-induced cell detah and cell cycle arrest. Future Virol. **5**:731–741.

58. **Chen AY, Luo Y, Cheng F, Sun Y, Qiu J.** 2010. Bocavirus infection induces a mitochondrion-mediated apoptosis and cell cycle arrest at G2/M-phase. J. Virol. **84**:5615–5626.

59. **Berthet C, Raj K, Saudan P, Beard P.** 2005. How adeno-associated virus Rep78 protein arrests cells completely in S phase. Proc. Natl. Acad. Sci. U. S. A. **102**:13634–13639.